Solid-State Effects in Spin Transitions: Role of Iron(II) Dilution in the Magnetic and Calorimetric Properties of the Series $[Fe_xNi_{1-x}(4,4'\text{-bis}(1,2,4\text{-triazole}))_2(NCS)_2]\cdot H_2O$

Jean-Pierre Martin,[1a] Jacqueline Zarembowitch,*[,1a] Ary Dworkin,[1b] Jaap G. Haasnoot,[1c] and Epiphane Codjovi[1a]

Laboratoire de Chimie Inorganique (CNRS, URA 420) and Laboratoire de Chimie Physique des Matériaux Amorphes (CNRS, URA 1104), Université de Paris-Sud, 91405 Orsay, France, and Gorlaeus Laboratories, Leiden University, P.O. Box 9502, 2300 RA Leiden, The Netherlands

Received September 16, 1993[⊗]

The effects of metal dilution on the spin-crossover behavior of $[Fe(btr)_2(NCS)_2]\cdot H_2O$ (btr = 4,4′-bis(1,2,4-triazole)) have been studied in the mixed-crystal series $[Fe_xNi_{1-x}(btr)_2(NCS)_2]\cdot H_2O$, using magnetic and calorimetric measurements. These compounds have a two-dimensional structure, and the thermally-induced spin-crossover process may present a hysteresis effect. Iron(II) dilution tends to smooth the transition curves. Moreover, when x changes from 1.00 to 0.26, the transition temperature varies from 121 to 132 K in the cooling mode and from 145 to 132 K in the heating mode. The hysteresis, which is 24 K for $x = 1.00$, vanishes for $x \approx 0.45$. No residual low-spin (high-spin) fraction is observed at room (very low) temperature. The enthalpy (entropy) change associated with the spin conversion of 1 mol of iron(II) mononuclear complex decreases from 10.2 kJ·mol^{-1} (76.4 J·mol^{-1}·K^{-1}) for $x = 1.00$ to 3.6 kJ·mol^{-1} (27.5 J·mol^{-1}·K^{-1}) for $x = 0.26$. These effects were interpreted first qualitatively, and then quantitatively, on the basis of a thermodynamic model, taking into account the relative sizes of Ni(II), high-spin Fe(II), and low-spin Fe(II) ions.

Introduction

In a number of transition-metal molecular compounds, the metal ion (with a d^4 to d^7 electronic configuration for an octahedral environment) is known to exhibit a high-spin state (HS) ↔ low-spin state (LS) crossover. This occurs when the ligand field strength is comparable in magnitude with the mean spin-pairing energy. The control parameter of the phenomenon may be temperature, pressure, or light. In such systems, the HS and LS states may coexist, their ratio varying as a function of the applied perturbation. The thermally-induced HS ↔ LS transitions are more or less cooperative. In liquid solutions, the spin-crossover behavior can be described by a Gibbs–Boltzmann distribution over the vibronic levels of the HS and LS states. In the solid state, the existence of intermolecular interactions leads to a large variety of transitions, going from very gradual to discontinuous ones;[2-11] the latter may present a thermal hysteresis effect.

An interesting way to know more about these interactions is to progressively move the spin-crossover molecules away from each other by diluting them, in the solid state, with an isomorphous compound retaining the same spin state over the scanned temperature range.[12-27]

Such studies have been previously performed on the iron(III) mixed complexes $[Fe_xM_{1-x}(3\text{-}OCH_3\text{-SalEen})_2]PF_6$ (where 3-OCH_3-SalEen is the monoanion of the Schiff-base resulting from the 1:1 condensation of 3-methoxysalicylaldehyde with *N*-ethylethylenediamine) with M = Co(III) or Cr(III) ions[14-16] and on the iron(II) mixed complexes $Fe_xM_{1-x}(Phen)_2(NCS)_2$ (where Phen = 1,10-phenanthroline) with M = Co(II), Ni(II), Mn(II), or Zn(II) ions[17] and $[Fe_xM_{1-x}(2\text{-pic})_3]Cl_2\cdot EtOH$ (where 2-pic = 2-picolylamine) with M = Co(II) or Zn(II).[18-27] The elastic character of the intermolecular interactions has been taken into account to interpret some of these data.[18-20] It should be noted that, to date, the effects of metal dilution have not yet been investigated on a compound exhibiting a spin transition with hysteresis.

We examined the case of the mixed species $[Fe_xNi_{1-x}(btr)_2(NCS)_2]\cdot H_2O$[28-31] (abbreviated as $[Fe_xNi_{1-x}]$), where btr stands for 4,4′-bis(1,2,4-triazole). The pure iron(II) complex

⊗ Abstract published in *Advance ACS Abstracts,* May 1, 1994.

(1) (a) Laboratoire de Chimie Inorganique, Université de Paris-Sud. (b) Laboratoire de Chimie Physique des Matériaux Amorphes, Université de Paris-Sud. (c) Gorlaeus Laboratories, Leiden University.
(2) Gütlich, P. *Struct. Bonding* **1981**, *44*, 83.
(3) König, E.; Ritter, G.; Kulshreshtha, S. K. *Chem. Rev.* **1985**, *85*, 219.
(4) König, E. *Prog. Inorg. Chem.* **1987**, *35*, 527.
(5) Beattie, J. K. *Adv. Inorg. Chem.* **1988**, *32*, 1.
(6) Bacci, M. *Coord. Chem. Rev.* **1988**, *86*, 245.
(7) Toftlund, H. *Coord. Chem. Rev.* **1989**, *67*, 108.
(8) Gütlich, P.; Hauser, A. *Coord. Chem. Rev.* **1990**, *97*, 1.
(9) Hauser, A. *Coord. Chem. Rev.* **1991**, *111*, 275.
(10) König, E. *Struct. Bonding* **1991**, *76*, 51.
(11) Zarembowitch, J. *New J. Chem.* **1992**, *16*, 255.
(12) Zelentsov, V. V.; Gabdrakhmanov, M. N.; Sobolev, S. S. *Khim. Fiz.* **1986**, *5*, 1216.
(13) Kambara, T. *J. Phys. Soc. Jpn.* **1980**, *49*, 1806.
(14) Hendrickson, D. N.; Haddad, M. S.; Federer, W. D.; Lynch, M. W. *(IUPAC) Coordination Chemistry-21*; Laurent, J. P., Ed.; Pergamon Press: Oxford and New York, 1981; p 75.
(15) Haddad, M. S.; Federer, W. D.; Lynch, M. W.; Hendrickson, D. N. *J. Am. Chem. Soc.* **1980**, *102*, 1468.
(16) Haddad, M. S.; Federer, W. D.; Lynch, M. W.; Hendrickson, D. N. *Inorg. Chem.* **1981**, *20*, 131.
(17) Ganguli, P.; Gütlich, P.; Müller, E. W. *Inorg. Chem.* **1982**, *21*, 3429.
(18) Spiering, H.; Meissner, E.; Köppen, H.; Müller, E. W.; Gütlich, P. *Chem. Phys.* **1982**, *68*, 65.
(19) Sanner, I.; Meissner, E.; Köppen, H.; Spiering, H.; Gütlich, P. *Chem. Phys.* **1984**, *86*, 227.
(20) Adler, P.; Wiehl, L.; Meissner, E.; Köhler, C. P.; Spiering, H.; Gütlich, P. *J. Phys. Chem. Solids* **1987**, *48*, 517.
(21) Rao, P. S.; Reuveni, A.; McGarvey, B. R.; Ganguli, P.; Gütlich, P. *Inorg. Chem.* **1981**, *20*, 204.
(22) Rao, P. S.; McGarvey, B. R.; Ganguli, P. *Inorg. Chem.* **1981**, *20*, 3682.
(23) Sorai, M.; Ensling, J.; Gütlich, P. *Chem. Phys.* **1976**, *18*, 199.
(24) Gütlich, P.; Link, R.; Steinhauser, H. G. *Inorg. Chem.* **1978**, *17*, 2509. Gütlich, P.; Köppen, H.; Link, R.; Steinhauser, H. G. *J. Chem. Phys.* **1979**, *70*, 3977.
(25) Jakobi, R.; Spiering, H.; Wiehl, L.; Gmelin, E.; Gütlich, P. *Inorg. Chem.* **1988**, *27*, 1823.
(26) Köhler, C. P.; Jakobi, R.; Meissner, E.; Wiehl, L.; Spiering, H.; Gütlich, P. *J. Phys. Chem. Solids* **1990**, *51*, 239.
(27) Jakobi, R.; Spiering, H.; Gütlich, P. *J. Phys. Chem. Solids* **1992**, *53*, 267.
(28) Vreugdenhil, W.; Van Diemen, J. H.; De Graaf, R. A. G.; Haasnoot, J. G.; Reedijk, J.; Van der Kraan, A. M.; Kahn, O.; Zarembowitch, J. *Polyhedron* **1990**, *9*, 2971.
(29) Vreugdenhil, W.; Gorter, S.; Haasnoot, J. G.; Reedijk, J. *Polyhedron* **1985**, *4*, 1769.
(30) Vreugdenhil, W.; Haasnoot, J. G.; Kahn, O.; Thuéry, P.; Reedijk, J. *J. Am. Chem. Soc.* **1987**, *109*, 5272.

0020-1669/94/1333-2617$04.50/0

Table 1. Elemental Analysis Data (%) and Molecular Weights (g) for the Mixed-Crystal Complexes $[Fe_xNi_{1-x}(btr)_2(NCS)_2]\cdot H_2O$

		anal: found (calcd)					
x	M_x	C	H	N	S	Fe	Ni
1.00	462.26	26.02 (25.96)	2.03 (2.16)	42.22 (42.40)	14.02 (13.85)	11.52	0.00
0.95	462.35	26.05 (25.95)	1.99 (2.16)	42.54 (42.39)	14.07 (13.84)	11.33	0.29
0.85	462.69	26.21 (25.93)	2.05 (2.16)	42.90 (42.36)	13.91 (13.83)	9.90	1.84
0.68	463.15	26.23 (25.91)	2.05 (2.15)	41.80 (42.31)	13.98 (13.81)	8.12	3.77
0.55	463.55	26.12 (25.88)	2.05 (2.15)	42.11 (42.28)	13.96 (13.80)	6.45	5.61
0.42	463.92	26.13 (25.86)	2.00 (2.15)	42.14 (42.24)	13.92 (13.79)	4.87	7.13
0.26	464.38	26.13 (25.84)	2.04 (2.15)	42.11 (42.20)	13.61 (13.78)	3.09	9.13
0.15	464.69	25.96 (25.82)	2.03 (2.15)	41.15 (42.17)	13.82 (13.77)	1.85	10.63
0.08	464.89	25.97 (25.81)	2.09 (2.15)	41.59 (42.16)	13.85 (13.76)	1.01	11.66
0.00	465.12	25.61 (25.80)	2.10 (2.15)	41.87 (42.14)	13.86 (13.76)	0.00	12.86

$[Fe(btr)_2(NCS)_2]\cdot H_2O$, [Fe], exhibits a very sharp spin transition (80% of the spin change occurs within 3 K) with a wide hysteresis of 24 K ($T_c\downarrow$ = 121 K and $T_c\uparrow$ = 145 K, $T_c\downarrow$ and $T_c\uparrow$ being the temperatures at which the HS fraction, n_{HS}, is equal to 0.5 in the cooling mode and the heating mode, respectively). The crystal structure of this compound, determined by X-ray diffraction,[29,30] is quite special. It consists of layers of six-coordinate iron(II) ions, the water molecules lying between the planes. Each [Fe] mononuclear entity includes two *trans*-orientated Fe–N(CS) bonds and is linked to four similar neighbors through single bridges of bis(triazole) in the equatorial plane, thus forming a two-dimensional network. The layers are connected to each other by means of van der Waals forces and weak hydrogen-bond bridges involving the water molecules. As there is only one water molecule for two bis(triazole) ligands, each of them including two noncoordinating nitrogen atoms, only half of the free electron pairs of these nitrogen atoms take part in hydrogen bonding. It should be noted that $[Fe(btr)_2(NCS)_2]\cdot H_2O$ is the first two-dimensional compound known to exhibit a spin transition. Given the structure, the interactions are expected to propagate mainly through the bridging ligands but also through the hydrogen bonds. X-ray photographs of $[Fe(btr)_2(NCS)_2]\cdot H_2O$ and $[Ni(btr)_2(NCS)_2]\cdot H_2O$ (referred to as [Ni]) show that these compounds are isomorphous.

Owing to the special characteristics of $[Fe(btr)_2(NCS)_2]\cdot H_2O$ (highly cooperative thermally-induced spin transition with hysteresis, two-dimensional structure), this compound proves to be particularly attractive for studying dilution effects. The experimental investigation of the mixed species $[Fe_xNi_{1-x}]$ we present in this paper is based on variable-temperature magnetic susceptibility measurements and on a differential scanning calorimetry (DSC) analysis. An adaptation of the phenomenological model of Slichter and Drickamer[32] has been developed to account for the data. This approach leads to a good description of gradual spin crossovers and of discontinuous spin transitions *with hysteresis*. It suits well the spin transition of $[Fe(btr)_2(NCS)_2]\cdot H_2O$.

Experimental Section

Materials. The preparation of 4,4′-bis(1,2,4-triazole) has been described earlier.[33] The synthesis of the pure compounds $[Fe(btr)_2(NCS)_2]\cdot H_2O$ and $[Ni(btr)_2(NCS)_2]\cdot H_2O$ consists in reacting the metal salt ($FeCl_2\cdot 4H_2O$ or $NiCl_2\cdot 4H_2O$), the bis(triazole) ligand, and ammonium thiocyanate in water around 70 °C.[28,29] Crystals were obtained by slowly cooling a hot (70 °C) solution of the reactants to room temperature. The diluted compounds $[Fe_xNi_{1-x}]$ were synthesized according to the same procedure, replacing the metal salt by mixtures of iron(II) chloride and nickel(II) chloride in given ratios.[30] Elemental analysis data are listed in Table 1.

Iron fraction (x) values were calculated from the iron and nickel concentrations (c_{Fe} and c_{Ni}) determined by elemental analysis. For a given compound, c_{Fe}, c_{Ni}, and the molecular weight M_x can be expressed as

$$M_x = xM_{Fe} + (1-x)M_{Ni} + M_L \quad (1)$$

$$c_{Fe} = \frac{xM_{Fe}}{M_x} \quad (2)$$

$$c_{Ni} = \frac{(1-x)M_{Ni}}{M_x} \quad (3)$$

where x and M_x are the two unknown quantities, M_{Fe} and M_{Ni} are iron and nickel atomic weights, and M_L represents the ligand molecular weight. The three possible x values obtained by combining these equations two by two were found to agree within ±2–3%. So x was estimated as their average. The x values thus determined deviate from those expected according to the relative amounts of the metal salts used for the syntheses. The discrepancies between the found and calculated values can be estimated from Figure 1.

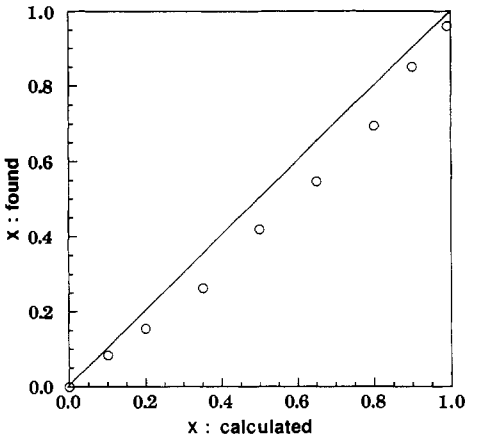

Figure 1. Iron fraction obtained from elemental analysis vs iron fraction calculated from the relative amounts of metallic salts used for the synthesis. The full line corresponds to the hypothetical situation where x found = x calculated.

Table 2. $\chi_{Fe}T$ Values at Room Temperature for Various $[Fe_xNi_{1-x}]$ Compounds

x	$\chi_{Fe}T$ (cm³·mol⁻¹·K)	x	$\chi_{Fe}T$ (cm³·mol⁻¹·K)
1.00	3.63	0.55	3.73
0.95	3.81	0.42	3.98
0.83	3.79	0.26	3.79
0.68	3.85		

Magnetic Measurements. The temperature dependence of the magnetic susceptibility was determined with a Faraday-type magnetometer equipped with an Oxford Instruments helium continuous-flow cryostat. The independence of the susceptibility with regard to the applied magnetic field was checked for each compound at room temperature. $HgCo(NCS)_4$ was used as a susceptibility standard. Diamagnetic corrections were estimated at -150×10^{-6} cm³·mol⁻¹ for all compounds. Temperature was varied at the rate of 1 K·min⁻¹ in the cooling mode and ≈0.5 K·min⁻¹ in the heating mode. The sample mass was typically ≈5 mg. As the [Fe] compound easily looses its water molecule and is, after that, in the high-

(31) Ozarowski, A.; Shunzhong, Y.; MacGarvey, B. R.; Mislankar, A.; Drake, J. E. *Inorg. Chem.* **1991**, *30*, 3167.
(32) Slichter, C. P.; Drickamer, H. G. *J. Chem. Phys.* **1972**, *56*, 2142.
(33) Haasnoot, J. G.; Groeneveld, W. L. *Z. Naturforsch.* **1979**, *34b*, 1500.

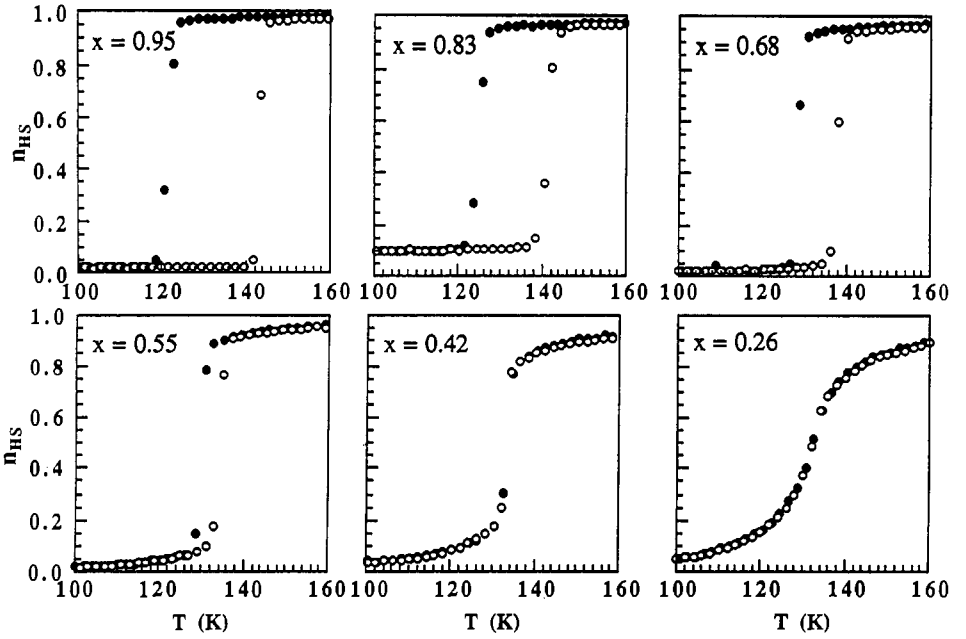

Figure 2. n_{HS} vs T curves for different x values, obtained from magnetic susceptibility measurements in the cooling (●) and heating (○) modes.

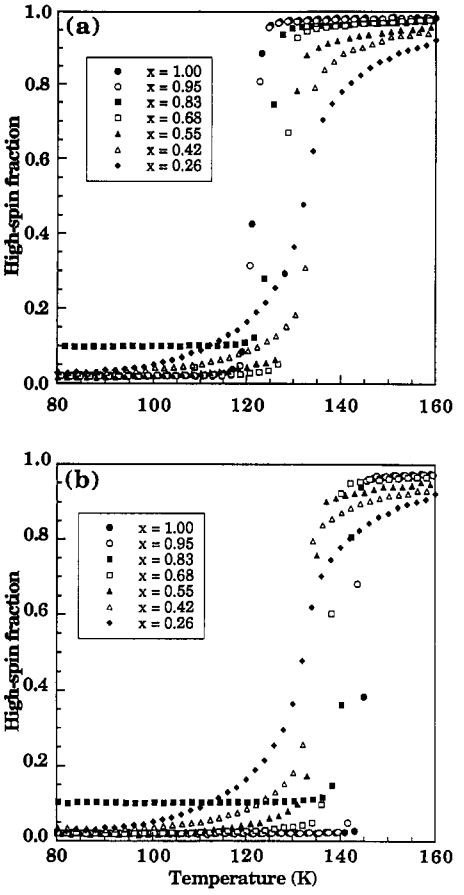

Figure 3. Evolution as a function of x of the n_{HS} vs T curves obtained (a) in the cooling mode and (b) in the heating mode from magnetic susceptibility measurements.

spin state at any temperature,[28,29,31] we designed a method to prevent the removal of water during the experiments: samples were submitted to primary vacuum at 160 K for 1 min; then they were kept under helium atmosphere at a pressure of ≈1 bar). Thermogravimetric analysis was used to check the presence of the expected amount of water in the samples after the experiments were completed.

DSC Measurements. The differential scanning calorimetry analysis was conducted on a Perkin-Elmer DSC-2 instrument, the low temperature attachment of which was a homemade cooling system allowing the temperature to be lowered to 83 K.[34] Helium was used as the purge gas. Sealed sample pans were employed. Temperature and enthalpy were calibrated with a sample of cyclohexane, using its melting (279.69 K and 2670 J·mol^{-1}) and crystal to crystal (186.70 K and 6740 J·mol^{-1}) transitions. Temperature values are known with a ±0.5 K accuracy, and enthalpies were determined with an experimental uncertainty of ±2% for a scan rate of 10 K·min^{-1}. The sample mass was between 5 and 10 mg.

Results

Magnetic Data. From magnetic susceptibility measurements, we determined the evolution of the $\chi_{exp}T$ product as a function of temperature (χ_{exp} = measured magnetic susceptibility for 1 mol of mononuclear entities and T = temperature). $\chi_{exp}T$ is the sum of the contributions of iron(II) ions and nickel(II) ions:

$$\chi_{exp}T = x\chi_{Fe}T + (1-x)\chi_{Ni}T \quad (4)$$

It follows that $\chi_{Fe}T$, which is relative to 1 mol of [Fe] entities, can be estimated from

$$\chi_{Fe}T = \frac{\chi_{exp}T - (1-x)\chi_{Ni}T}{x} \quad (5)$$

Since iron(II) ions in the LS state are diamagnetic, this product is proportional to the HS fraction. For low iron(II) concentrations, $\chi_{exp}T$ is close to $(1-x)\chi_{Ni}T$, which leads to a limit in the determination of iron(II) contribution. $\chi_{Fe}T$ values can be considered reliable only when x values are higher than ≈0.25.

The HS fraction (n_{HS}) at a given temperature was obtained by dividing the $\chi_{Fe}T$ value by the asymptotic value of the $\chi_{Fe}T$ vs T curve at room temperature (which was found not to depend on x within the experimental error (±≈5%), as shown in Table 2).

Figure 2 shows the evolution of n_{HS} as a function of temperature, in the cooling and heating modes, for several mixed compounds. When x decreases, (i) spin-crossovers become globally more gradual, though they still present a discontinuity around the point of inflexion for x as low as 0.42, (ii) the hysteresis width gets narrower and cancels out for $x \approx 0.45$, and (iii) no significant LS (HS) residual fraction is observed at room (very low) temperature. The noticeable amount of HS form found at low temperature for the sample with $x = 0.83$ results from the loss of a little water during the magnetism experiment.

(34) Dworkin, A.; Szwarc, H. *High Temp.-High Pressures* **1989**, *21*, 195.

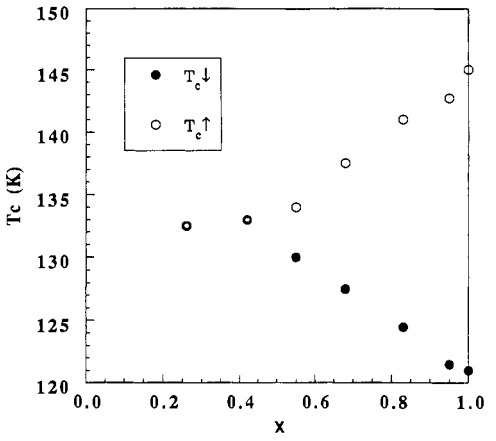

Figure 4. Evolution as a function of x of the transition temperatures T_c in the cooling (●) and heating (○) modes.

In Figure 3, where are collected the n_{HS} vs T curves obtained for all the compounds between 80 and 160 K in the cooling mode (Figure 3a) and in the heating mode (Figure 3b), the three above-described dilution effects are clearly evidenced. In particular, when x diminishes, $T_c\downarrow$ and $T_c\uparrow$ are found to increase and to decrease, respectively, and then to reach the same limit, which accounts for the reduction and the vanishing of the hysteresis loop. This effect is detailed in Figure 4. When x changes from 1.00 to 0.26, $T_c\downarrow$ varies from 121 to 132 K and $T_c\uparrow$ from 145 to 132 K. The hysteresis, which is 24 K for $x = 1.00$, vanishes for $x \approx 0.45$. If we assume, as a first approximation, that T_c corresponds to $(T_c\downarrow + T_c\uparrow)/2$, it appears that the value of T_c is constant whatever x may be ($T_c = 132$ K).

DSC Data. On the thermograms, the peak area corresponds to an enthalpy. The enthalpy changes ΔH_{exp}, associated with the spin conversion of the mass unit of the $[Fe_xNi_{1-x}]$ complexes, were directly obtained from the DSC data processing program. This allowed us to calculate the quantities ΔH relative to the spin conversion of 1 mol of [Fe] entities, using the following relation:

$$\Delta H = \frac{\Delta H_{exp} M_x}{x} \qquad (6)$$

The relevant entropy changes ΔS were determined from $\Delta S = \Delta H/T_c$. Experimental errors on ΔH increase with dilution, going from about 5% for $x = 1$ to about 30% for $x = 0.26$. Errors on ΔS are somewhat larger.

Figure 5 shows thermograms related to the same mass of various $[Fe_xNi_{1-x}]$ complexes, obtained between 110 and 160 K in the heating mode. When x decreases, the peaks shift toward low temperatures. Below $x \approx 0.2$, they could not be distinguished from the background noise.

The evolution of ΔH with x is shown in Figure 6. This enthalpy variation remains constant ($\approx$10.0 kJ·mol^{-1}) for $0.7 \leq x \leq 1.0$ and then continuously decreases to 3.6 kJ·mol^{-1} for $x = 0.26$. The entropy change ΔS presents a similar behavior (see Figure 7): it does not vary significantly from $x = 1.0$ to $x = 0.7$, being close to 80 J·mol^{-1}·K^{-1}, and then decreases to 27 J·mol^{-1}·K^{-1} for $x = 0.26$.

Influence of the Size of the Metal Ions

As seen above, when the iron concentration decreases, the spin-crossover of $[Fe_xNi_{1-x}]$ species becomes globally more gradual, which is indicative of a progressive loss of cooperativity, and the hysteresis loop gets narrower nearly symmetrically on both sides of a given T_c value (132 K) and then vanishes. No residual fraction is observed either at low temperature or at 293 K. Finally, the enthalpy and entropy changes associated with the transformation of 1 mol of [Fe] entities, ΔH and ΔS, are found to depend on x.

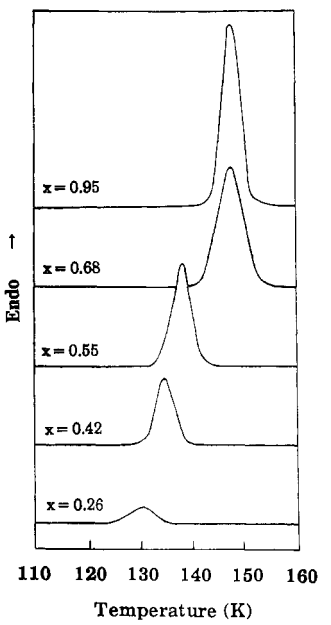

Figure 5. DSC curves obtained for different x values in the heating mode. All of them refer to the spin conversion of the same mass of $[Fe_xNi_{1-x}]$ mixed complex. For clarity, the curves have been translated vertically.

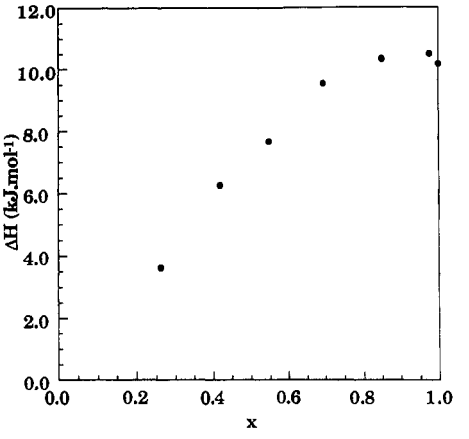

Figure 6. Evolution as a function of x of the transition enthalpy relative to 1 mol of [Fe] entities.

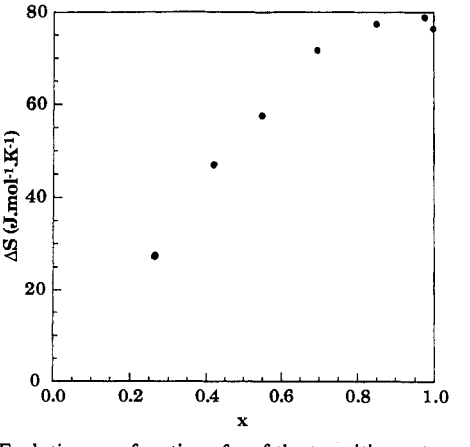

Figure 7. Evolution as a function of x of the transition entropy relative to 1 mol of [Fe] entities.

The direct effects of dilution fall into two categories: (i) increase in the distances between iron ions; (ii) development of interactions between [Fe] and [Ni] entities.

The former effect can be estimated by determining the probability for a given iron ion to be surrounded by **q** similar ions. Figure 8, which shows the evolution of this probability as a function

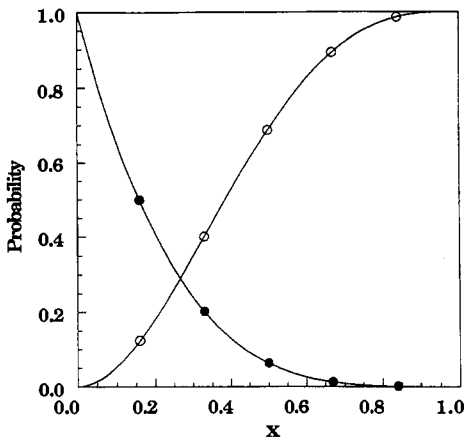

Figure 8. Probability for the number of [Fe] entities surrounding a given [Fe] entity to be 0 (●) or at least 2 (○).

of x for $\mathbf{q} = 0$ and $\mathbf{q}$ = at least 2, has been drawn taking into account the fact that each [Fe] entity is directly bound, through the bridging ligands, to four [Fe] or [Ni] first neighbors. For the situation $\mathbf{q} = 0$ to occur with a probability of 0.9, x has to be as low as 0.03. When $x = 0.15$, only 50% of the molecules are still in this situation. Thus, very low x values are required for the [Fe] groups to be actually considered isolated. On the other hand, as soon as $x > 0.4$, more than half of the iron(II) ions have two iron neighbors at least.

Regarding the latter dilution effect, i.e. the development of interactions between the spin-crossover and the diluting ions, the influence of the relative sizes of these ions has been pointed out by Hendrickson et al.[14-16] and Ganguli et al.[23] Now, the ionic radius of HS nickel(II) ($\mathbf{r} = 83$ pm) is nearly half way between the ionic radii of HS ($\mathbf{r} = 92$ pm) and LS ($\mathbf{r} = 75$ pm) iron(II).

If iron(II) ions are highly diluted in a [Ni] lattice, two cases have to be distinguished. When these ions are in the HS state, they are bulkier than nickel(II) ions and, consequently, subjected to a positive pressure from their surrounding: the LS form is then stabilized. When the iron(II) ions are in the LS state, they are smaller than nickel(II) ions, and the negative pressure produced by their environment stabilizes the HS form. Thus, in both cases, the primary dilution effect is a destabilization of the initial spin state. However, the difference in ionic radius between Fe(II) and Ni(II) ions being 9 pm if iron(II) is in the HS state and 8 pm if it is in the LS state, the Fe_{HS}/Ni and Fe_{LS}/Ni interaction amplitudes must be of the same order of magnitude. So, the influence of the environment on the modified iron ions should compensate the first effect and lead finally to an unchanged spin state. It follows that no residual fraction is expected to exist at very low or room temperature, which is actually observed.

Thermodynamic Approach

Basic Equations. The experimental results were accounted for on the basis of the model of Slichter and Drickamer[32] we have adapted to diluted compounds. In this model, the Gibbs free energy of an assembly of N_A spin-crossover molecules (N_A = Avogadro's number) characterized by the HS fraction n_{HS} is expressed as that of a strictly regular solution:

$$G = n_{HS}G^\circ_{HS} + (1 - n_{HS})G^\circ_{LS} + n_{HS}(1 - n_{HS})\Gamma - TS_{mix} \quad (7)$$

where G°_{HS} and G°_{LS} are the molar standard Gibbs free energies of the HS and LS forms, respectively, Γ is an interaction parameter and S_{mix} is the mixing entropy of the HS and LS entities, which can be written as

$$S_{mix} = -R[n_{HS}\ln(n_{HS}) + (1 - n_{HS})\ln(1 - n_{HS})] \quad (8)$$

In the mixed compounds $[Fe_xNi_{1-x}]$, N_A mononuclear entities contain: (i) xN_A [Fe] groups, including $xn_{HS}N_A$ groups in the HS state and $x(1 - n_{HS})N_A$ groups in the LS state; (ii) $(1 - x)N_A$ [Ni] groups.

The Gibbs free energy is then given by

$$G = xn_{HS}G^\circ_{HS} + x(1 - n_{HS})G^\circ_{LS} + (1 - x)G^\circ_{Ni} + x^2n_{HS}(1 - n_{HS})\Gamma + x(1 - x)n_{HS}\Gamma_{HS/Ni} + x(1 - x)(1 - n_{HS})\Gamma_{LS/Ni} - xn_{HS}TS_v^{HS}(x) - x(1 - n_{HS})TS_v^{LS}(x) - TS_{mix} \quad (9)$$

G°_{HS}, G°_{LS}, and G°_{Ni} are the standard Gibbs free energies of N_A $[Fe]_{HS}$ or $[Fe]_{LS}$ entities (in which iron(II) is in the HS state and the LS state, respectively) and N_A [Ni] entities. Γ, $\Gamma_{HS/Ni}$, and $\Gamma_{LS/Ni}$ are parameters of enthalpic origin, accounting for the interactions between the groups $[Fe]_{HS}$ and $[Fe]_{LS}$, $[Fe]_{HS}$ and [Ni], and $[Fe]_{LS}$ and [Ni], respectively.

The additional entropy terms S_v^{HS} and S_v^{LS}, associated with the presence of nickel ions, represent the differences between the entropies of vibrational origin relative to N_A $[Fe]_{HS}$ or $[Fe]_{LS}$ entities, respectively, in the pure and the mixed systems. These differences result from the fact that the coupling between the vibrational modes of neighboring [Fe] groups, which mainly occurs within the equatorial plane, is modified by the presence of [Ni] groups, leading to changes in the vibrational frequencies, and hence in the corresponding entropies.

Finally, S_{mix} stands for the mixing entropy of all the species and is defined by

$$S_{mix} = -R[xn_{HS}\ln(xn_{HS}) + x(1 - n_{HS})\ln\{x(1 - n_{HS})\} + (1 - x)\ln(1 - x)] \quad (10)$$

In the following development, eq 9 can be replaced (according to eq 17) by eq 11, where the terms which do not depend on n_{HS} have been omitted:

$$G' = xn_{HS}[\Delta H^\circ - T\Delta S^\circ] + x^2n_{HS}(1 - n_{HS})\Gamma + x(1 - x)n_{HS}\Gamma_M - xn_{HS}T\Delta S_v(x) - TS_{mix} \quad (11)$$

Here, ΔH° and ΔS° are the standard enthalpy and entropy variations associated with the spin conversion of N_A [Fe] entities in the pure iron compound and

$$\Gamma_M = \Gamma_{HS/Ni} - \Gamma_{LS/Ni} \quad (12)$$

$$\Delta S_v(x) = S_v^{HS}(x) - S_v^{LS}(x) \quad (13)$$

Equation 11 can also be written as

$$G' = xn_{HS}[\Delta H(x) - T\Delta S(x)] + x^2n_{HS}(1 - n_{HS})\Gamma - TS_{mix} \quad (14)$$

where

$$\Delta H(x) = \Delta H^\circ + (1 - x)\Gamma_M \quad (15)$$

$$\Delta S(x) = \Delta S^\circ + \Delta S_v(x) \quad (16)$$

Equation 14 compares with the corresponding Slichter and Drickamer equation (see eq 7), where G°_{LS} is taken as the energy origin and leads, when applying the equilibrium condition for the systems

$$\left(\frac{\partial G}{\partial n_{HS}}\right)_{T,P,x} = \left(\frac{\partial G'}{\partial n_{HS}}\right)_{T,P,x} = 0 \quad (17)$$

to

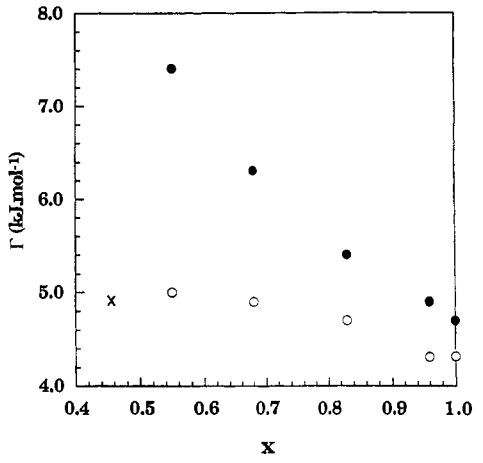

Figure 9. Evolution as a function of x of the interaction parameter Γ: (●) Γ values determined from eq 19, using $T_c\downarrow$ values; (○) Γ values determined from eq 19, using $T_c\uparrow$ values; (×) Γ value determined from eq 23.

$$\ln\left[\frac{1-n_{HS}}{n_{HS}}\right] = \frac{\Delta H(x) + x(1-2n_{HS})\Gamma}{RT} - \frac{\Delta S(x)}{R} \quad (18)$$

From this equation, it is easy to deduce the function

$$T = \frac{\Delta H(x) + x(1-2n_{HS})\Gamma}{\Delta S(x) + R\ln\left[\frac{1-n_{HS}}{n_{HS}}\right]} \quad (19)$$

and hence to get the evolution of n_{HS} as a function of T.

Evolution of the Parameters as a Function of Dilution. Let us now consider the variation of the parameters $\Delta H(x)$, $\Delta S(x)$, and Γ with iron concentration.

Enthalpy Variation: $\Delta H(x) = \Delta H^\circ + (1-x)\Gamma_M$. The preceding expression shows that the relative stability of the two spin isomers of iron(II), which depends on $\Delta H(x)$, is governed by Γ_M. If this parameter is positive, then the LS state is stabilized by dilution; on the contrary, if Γ_M is negative, then the HS state is stabilized. Now Γ_M is defined as $\Gamma_M = \Gamma_{HS/Ni} - \Gamma_{LS/Ni}$ (see eq 12), and the terms $\Gamma_{HS/Ni}$ and $\Gamma_{LS/Ni}$ are expected to depend on the difference between the ionic radii of the metal ions. The fact that this difference is of the same order of magnitude in the pairs Fe_{HS}/Ni and Fe_{LS}/Ni should then lead to

$$\Gamma_{HS/Ni} \approx \Gamma_{LS/Ni} \quad (20)$$

hence to

$$\Gamma_M \approx 0 \quad (21)$$

and, consequently, to

$$\Delta H(x) \approx \Delta H^\circ \approx \text{constant} \quad (22)$$

Figure 6 shows that this last property is observed for $0.7 \leq x \leq 1.0$. However, for $x < 0.7$, $\Delta H(x)$ is found to decrease significantly with x, which is likely to indicate that Γ_M is then negative. Such a behavior may be accounted for, at least partly, by a possible evolution of Γ_M as a function of x and/or by an experimental underestimation of $\Delta H(x)$ values, which is expected to be all the more pronounced as the dilution is higher.

Entropy Variation: $\Delta S(x) = \Delta S^\circ + \Delta S_v(x)$. The behavior of $\Delta S(x)$ for $x < 0.7$ (see Figure 7) suggests that $\Delta S_v(x)$ is then negative and becomes more and more important with increasing dilution. This is in agreement with the fact that, as seen above, this term mainly originates from the alteration of the coupling between [Fe] vibrational modes within the equatorial plane, induced by the presence of the nickel ions.

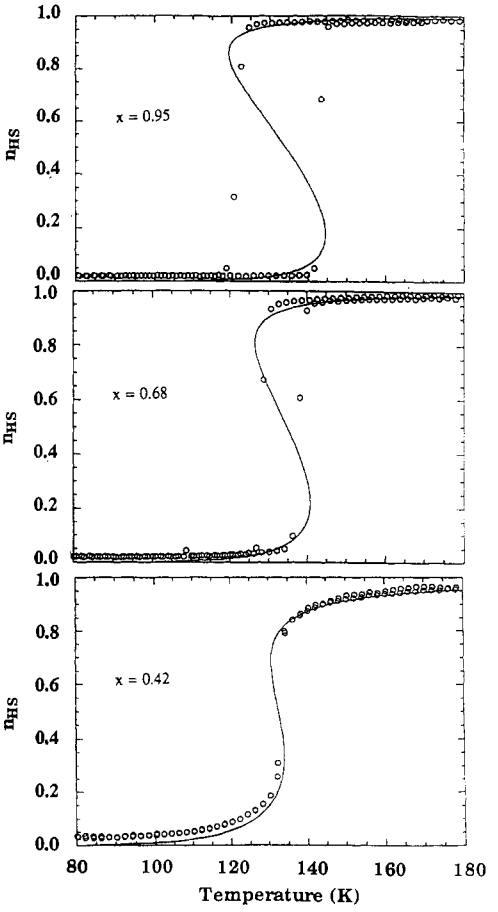

Figure 10. Experimental (○) and simulated (full lines) n_{HS} vs T curves for some representative x values.

Table 3. Values of the Interaction Parameter Γ Determined from the Simulation of the Experimental n_{HS} vs T Curves (Γ_1) and through Calculation from Eq 19 by Using the Values of $T_c\uparrow$ (Γ_2) and $T_c\downarrow$ (Γ_3)

x	Γ_1 (kJ·mol^{-1})	Γ_2 (kJ·mol^{-1})	Γ_3 (kJ·mol^{-1})
1.00	4.30	4.30	4.65
0.95	4.35	4.35	4.75
0.68	5.00	4.80	6.13
0.55	5.40	5.00	7.40

Interaction Parameter: Γ. The interaction term Γ can be calculated from eq 19, using the experimental values of $T_c\downarrow$ on the one hand and of $T_c\uparrow$ on the other hand. The evolution of this term as a function of x is shown in Figure 9. The values obtained from $T_c\uparrow$ only slightly vary, passing from 4.3 kJ·mol^{-1} for x = 1.0 to 5.0 kJ·mol^{-1} for x = 0.55, while those calculated with $T_c\downarrow$ increase from 4.65 kJ·mol^{-1} to 7.4 kJ·mol^{-1} between the same x values (see Table 3).

Γ values can also be deduced from the n_{HS} vs T curves obtained by magnetic susceptibility measurements. These curves can be quite properly simulated by eq 19, using DSC data and taking Γ as the unknown parameter (see Figure 10). The Γ values so determined are collected in Table 3. They are very close to those obtained through calculation with $T_c\uparrow$.

These two ways to estimate Γ lead to values which increase, more or less, with decreasing iron concentration (see Figure 9). This might be accounted for, at least partly, by the fact that the uncertainty on the experimental data grows rapidly with dilution.

Finally, a Γ value can be deduced from Figure 4, which shows that the hysteresis of the n_{Hs} vs T curves vanishes for $x \approx 0.45$. In the case of undiluted systems, it is easy to show[32] that such a situation occurs when $\Gamma = 2RT_c$. For mixed-crystal compounds, this relation becomes

$$x\Gamma = 2RT_c \quad (23)$$

which leads in the present case, taking x as 0.45, to Γ = 4.8 kJ·mol^{-1}. This value is also in agreement with the values estimated from $T_c\uparrow$ (see Figure 9).

Conclusion

According to the foregoing, the phenomenological model we developed to account for dilution effects in the [Fe_xNi_{1-x}] system proves to simulate the experimental n_{HS} vs T curves properly. This is likely to partly result from the fact that this model leads to spin-crossovers which are either *totally discontinuous with hysteresis* or *gradual without hysteresis*. Now, the pure [Fe] species exhibits a transition typically of the former type. Also, regarding the mixed compounds, the discontinuity of the transition curves around T_c remains pronounced down to the lowest x values for which a hysteresis effect is still observed: for x = 0.55, 60% of the spin change takes place within 2 K. Moreover, the Γ values obtained from the simulation of the curves, using the experimental values of enthalpy and entropy, are found to have a satisfying order of magnitude. So, this model appears to be well adapted to account for the dilution effects in the family of mixed compounds investigated.